THE COMMISSIONING OF THE CHEIA ROMANIAN RADAR SENSOR FOR SPACE SURVEILLANCE AND TRACKING

Liviu Ionescu [(1)], Alexandru Rusu-Casandra [(2)], Calin Bira [(2)], Alexandru Tatomirescu [(2)], Ionut Tramandan[(1)], Roberto Scagnoli[(1)], Dan Istriteanu[(1)] and Andrei-Edward Popa[(2)]

[(1)] RARTEL S.A., 011041 Bucharest, Romania, liviu.ionescu@rartel.ro
[(2)] Faculty of Electronics, Telecommunications and Information Technology, Politehnica University of Bucharest, 060042 Bucharest, Romania

ABSTRACT

The constant growth in the number of space objects and debris flying in various orbits around the Earth creates dangers to satellites and other space vehicles, both in orbit and during the launching process. Therefore, the tracking of space hazards to evaluate risk and prevent collisions is of high importance for human activity in space, but also due to the potential threat to people and assets on the ground. The European Space Policy for years 2021-2027 acknowledges this problem, includes a dedicated element for Space Situational Awareness (SSA) and requires the establishment of a Framework for Space Surveillance and Tracking (EUSST) Support. As part of this effort, a new space tracking sensor, the CHEIA SST Radar, has been developed and installed in Romania, with the purpose of detecting and tracking LEO objects. The present paper gives an overview and describes the functional processes of the Radar system. It also contains the initial results of the antenna pointing tests.

Keywords Space Situational Awareness, Space Surveillance and Tracking, Cheia Radar

1 INTRODUCTION

The Cheia Radar constitutes a particular case of space sensor because of using an already existing system of two large parabolic antennas requiring an innovative retrofitting design to include them as the basis for a new quasi-monostatic Radar using LFMCW probing signals. The existing Cheia 32m parabolic antennas (built in 1977 and 1979 respectively) were used in the past for telecommunication applications and are presently no longer in use. The preliminary design was validated by extensive simulations and the initial operational testing carried out in December 2021 demonstrated the good performance of the Radar in the measuring range and radial speed of LEO space objects. Section 2 gives an overview of the Cheia space Radar. In section 3 are explained the Radar functional processes. Section 4 contains the Radar antenna calibration procedure and initial results. The paper ends with conclusions.

2 OVERVIEW OF THE RADAR

The Cheia Radar block diagram is shown in Figure 1 [1]. It contains several components: Transmitter (Tx), Receivers (Rx), Antenna Control Units (ACU), Main Processing Unit (MPU) and other subsystems.

The Positioning Satellites Constellation (PSC) Controlled Master Oscillator (MO), the RF generator and the Solid State Power Amplifier (PA) are subsystems of the Tx The probing signals are generated by the RF Generator, a configurable and very low noise microwave generator, based on configuration commands received from the Main Processing Unit (MPU). The frequency stability of the survey signal is increased by using the external reference signal provided by the PSC Controlled Master Oscillator (MO). The survey signal generated by the RF Generator is amplified to the final power level (2.5 kW) in the Power Amplifier, a linear power amplifier, made with MOSFET transistors. The high power signal is then applied to the LHCP port of the antenna feeder and is radiated in the form of electromagnetic waves with left circular polarization (LHCP) by the transmission antenna (Tx Antenna).

A part is extracted from the emitted signal, to be used as a signal of the local oscillator (LO) in the receiver (Receiver). The LO signal is extracted from the RF Generator output through a coupler.

PSC Controlled Master Oscillator (MO), RF generator and Power Amplifier are the 3 subsystems of the transmitter (Transmitter (Tx)). The microwave generator (RF generator) generates the MLF CW probing signal together with a synchro signal (Pulse) synchronized with each slope of the triangular signal used for frequency modulation. To reduce the phase noise in the probing signal, the microwave generator uses a very good quality frequency synthesizer, synchronized by a very stable external reference of 100MHz.

The Radar works as a CW Radar but, providing the overcome of the current technical reliability limitations of the Solid State Power Amplifiers, it could work as a pulsed Radar (FH-P mode) as well. In CW mode, the “Pulse” commands the sampling start in the Signal Processors. In Frequency Hopping Pulsed (FH-P) mode,

Proc. 2nd NEO and Debris Detection Conference, Darmstadt, Germany, 24-26 January 2023, published by the ESA Space Safety Programme Office
Ed. T. Flohrer, R. Moissl, F. Schmitz (http://conference.sdo.esoc.esa.int, February 2023)

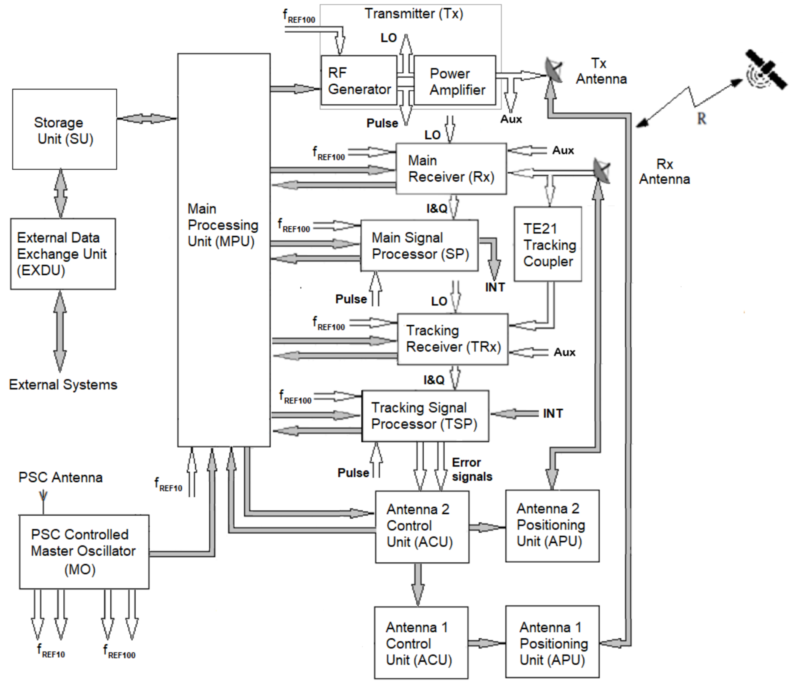

Figure 1 Cheia Radar block diagram

the "Pulse" commands the blocking of the power amplifier, in addition to the sampling start in the Signal Processors.

The echo signals are received at the RHCP port of the reception antenna feeder (Rx Antenna). Next, they are filtered, frequency translated/demodulated using the LO signal and amplified in the main channel receiver (Main Receiver), up to the level for the optimal operation of the analog-to-digital converter, part of the main channel signal processor, (SP). To compensate for the increase in phase noise and interference due to the coupling between the transmitting and receiving antennas or nearby objects, the main channel receiver, uses special signal processing techniques [2,3].

The Main Signal Processor translates the digital signal from the time domain to the frequency domain, applies time markers to it and processes it through a CFAR algorithm to extract target characteristics: slant range, Doppler velocity, and signal-to-noise ratio (SNR) which is an indicator of the size of the target. The data regarding the characteristics of the target extracted in the main channel is sent to the main processing unit, Main Processing Unit (MPU).

The main processing unit, Main Processing Unit (MPU), is an IT system that controls the operation of the Radar through a software application, M&C Software, based on microservices that send commands to the Radar subsystems [4]. The application contains algorithms grouped in three subsystems.

The first group, the group dedicated to the preparation of the tracking campaign, controls the stages of the preparation of the tracking campaign by processing the input data that designates the targets to be tracked. The algorithms of this group determine the visibility windows of the target, ensure their planning in sequence and establish the Radar parameters for tracking. This group is also responsible for storing the tracked target data in the Storage Unit.

The second group, the operational group, is intended to control the effective operation of the Radar, by loading the initial data of the target, by establishing the range scales as well as the distance and Doppler windows that will be used for tracking the target in range and Doppler. The group also establishes the method of angular tracking of the target. The decisions of the contained software algorithms can be based either on operator requests (manual tracking) or on operational criteria such as estimated orbital parameters, required/available accuracy, target size, received signal level, etc. In addition, the operational group of algorithms also ensures the consolidation of measurements in trajectories as well as their transformation according to the TDM standard. One of the group's algorithms tests the functionality of the Radar during tracking.

The third group, the group dedicated to maintenance, ensures the determination of subsystem errors and the setting of the configuration parameters of the whole Radar system.

The M&C application running on the MPU is a web application that has an architecture based on microservices. Each microservice is independent and has a behaviour specific to the equipment it serves. Each component of the Radar is paired with its dedicated microservice through M&C's configuration system. Being a web application, M&C allows operating the Radar both locally and remotely, through the same interface.

The movement of the Radar antennas (Tx Antenna and Rx Antenna) is controlled by two separate positioning systems, Antenna Positioning Systems (APS). Each APS is composed of an Antenna Control Unit (ACU) and an Antenna Positioning Unit (APU). The two APS are synchronized through a high-speed data link. When the Radar works in Programmed Tracking mode (on a predetermined path based on TLEs), both ACU units are controlled by the MPU. When the Radar works in Automatic Tracking mode, the control unit (ACU) of the receiving antenna is controlled by the error signals provided by the signal processor of the tracking channel, (TSP), while the antenna control unit (ACU) of the transmitting antenna is controlled by the ACU of the Rx antenna.

3 RADAR FUNCTIONAL PROCESSES

The Cheia Radar is designed for maximum flexibility, containing subsystems interconnected by a software algorithm, similar to configurable reception systems of the "software defined radio" type. The general operating algorithm of the Cheia Radar is presented in Figure 2.

The light blue blocks indicate the processing that takes place within the signal processor (MSP and TSP), separately indicating the processing within the main channel signal processor (MSP).

The light yellow block indicates the processing performed in the two computers of the antenna positioning system. It should be noted that the automatic target tracking process is performed in a closed loop only with the reception antenna, which is directly involved in the generation of angular error signals. The transmission antenna is repositioned according to the reception antenna by reading the position of the reception antenna and retransmitting its angular coordinates to the transmission antenna. The use of automatic target tracking allows improving the accuracy of determining the angular coordinates of the target.

Processing outside the three blocks is performed in the M&C application running on the MPU within the operational group of algorithms. The signal processor performs a transformation in the frequency domain, which allows the extraction of the signal from the noise in extremely unfavourable conditions of signal-to-noise ratio, conditions that are commonly found in space Radars. The Cheia Radar can work with very low signal-to-noise ratios at the output of the receiver, around -50dB, while a Radar that processes in the time domain needs a signal-to-noise ratio of around 13dB, i.e. 63dB higher.

Figure 3 details the signal processing algorithm of the main receiver channel. The essential component of the processing is the calculation of the Fast Fourier Transform (FFT), which actually ensures the translation of the echo signal from the time domain to the frequency domain. This is the method of choice for narrowing the instantaneous bandwidth of a Radar, considering that applying a Fast Fourier Transform of length N to a signal of bandwidth B, is equivalent to passing the signal through a set of N contiguous filters having a bandwidth of B/N each.

To maximize the FFT impact, the echo signal of a target is transformed into a signal with a very narrow spectrum (theoretically single frequency), while the noise affecting the echo signal occupies the entire receiver band, its power being the sum of the power of all its components which are available at all the frequencies in this band .

Figure 4 represents the samples from the time domain of an echo signal, with a frequency of 2 MHz, deeply embedded in noise, having a signal to noise ratio SNR=-40dB, similar to the signal received by the Cheia Radar from a small target.

Figure 5 represents the same signal after it has been translated in the frequency domain, using an FFT with size N= 131,072 points, while Figure 6 shows the same signal at the output of the Cheia Radar signal processor using an FFT with size N= 262,144 points. The emergence of the signal from the noise is clearly observed, as a result of the frequency translation through an FFT of adequate size.

Figures 5 and 6 show that, using a set of very narrow pass-band filters, the spectral components of the noise will be distributed in all the filters in the set, the noise power in each filter being further reduced as the band of a single filter is reduced, that is as the FFT size, N is increased. The echo signal will exist only in one filter, the one corresponding to the pair of Range-Doppler of the target. In this way, for an FFT of size N, or a set of N filters, the signal to noise ratio in the cell will increase N times. In the case presented in Figure 5, the signal to noise ratio increases by approximately 50dB.

Obviously, the set of filters must cover the band corresponding to the echo signal. In the case of the Cheia CW probing signal, the band in which the echo signal can be found is Δf_b=2.08MHz while in the case of pulses with MLF this band increases to $\Delta f'_b$=4.82 MHz.

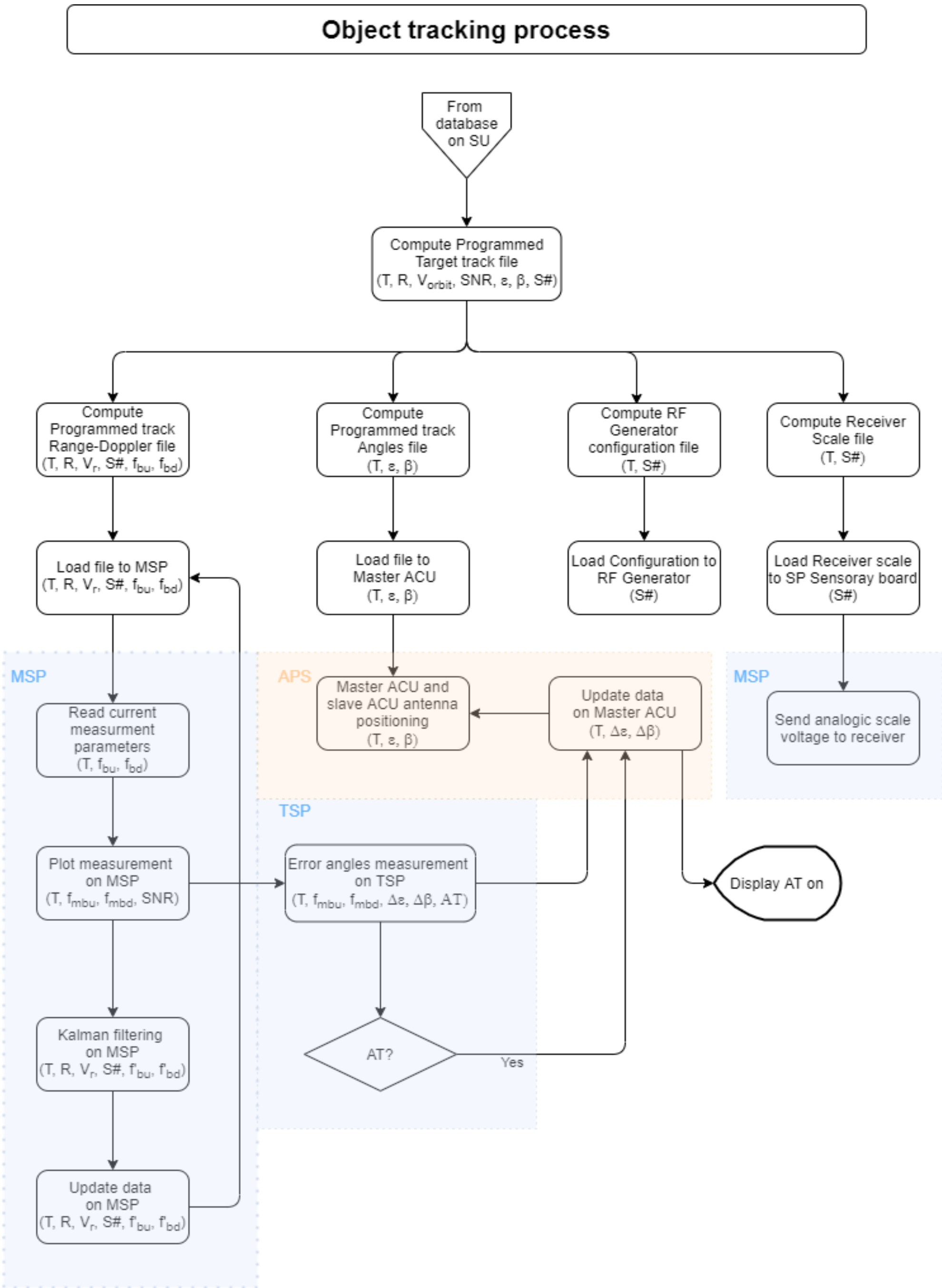

Figure 2 Flow diagram of the object tracking process

Applying a large FFT seems like a miraculous solution, but it also comes with a set of drawbacks. Thus, increasing the size of the FFT requires an exponential increase in computing resources, especially the required memory and the computing power. The calculation algorithm is relatively simple, but it requires the use of an extremely large number of multiplications in complex numbers. In addition, the size of the frequency cell (band of a filter) is inversely proportional to the duration of the transformed signal [5-7]l.

The detection requirement for Cheia Radar is:

$$d_{min} = max\left\{\sqrt{\frac{h_p^4}{h_{ref}^4}d_{ref}^2}, 1cm\right\} \quad (1)$$

The gain of the antennas of 63.5 dBi and the average transmitted power of 2.5 kW (34 dB).

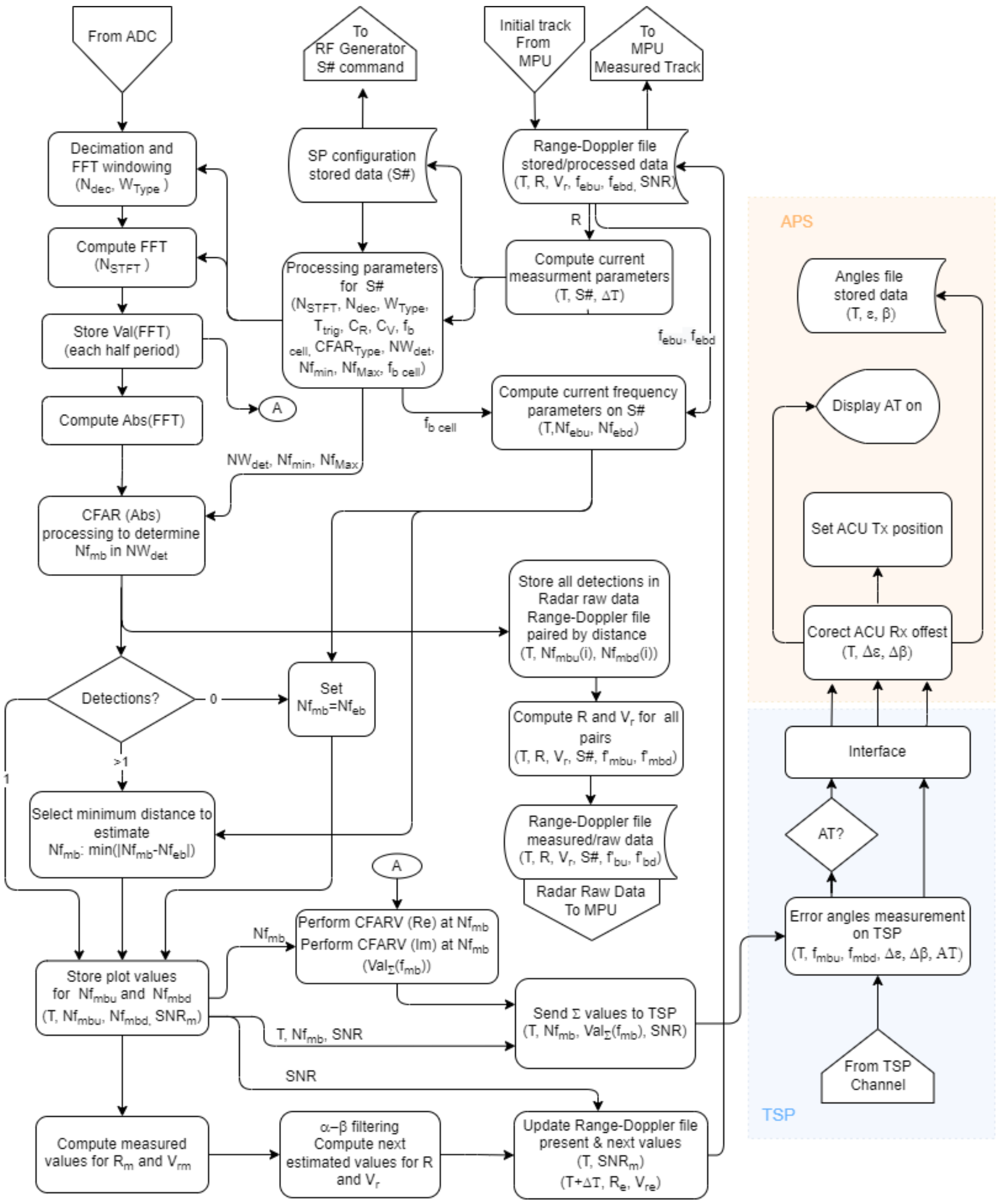

Figure 3 Flow diagram of main signal processor

Assuming the previously stated values, the value of the product:

$$P_{Tx} \cdot G_{Tx} \cdot G_{Rx} = (34 + 2 * 63.5)dB = 161dB \qquad (2)$$

allows the fulfilment of the detection requirements [8-10] in detected object size and altitude, if the receiver, following the signal processing, is able to provide an output SNR of:

$$SNR_{min} = 13.2dB \qquad (3)$$

(the Neyman-Pearson threshold for $P_d = 0.9$ and $P_{Fa} = 10^{-6}$), for a received C-band signal with the minimum power of:

$$P_{Rx\,min} = -148dBm \qquad (4)$$

To meet the previous requirements, the receiver must use an FFT that provides an instant bandwidth of:

$$B_{Rx} = 20Hz \qquad (5)$$

in the case of a coupling between transmission and reception of less than -105dB. In the case of a coupling greater than -105dB, additional phase noise reduction techniques should be used, the receiver's bandwidth should be reduced or the transmitter's phase noise should be reduced [11,12].

In order to provide a frequency band of 20 Hz when the bandwidth of the received signal is 2MHz, a FFT with the size of approx. N = 1,000,000 must be used and the duration of the window in which the signal must be stationary should be at least:

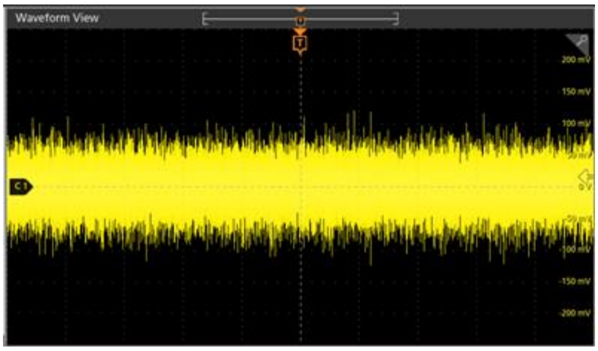

Figure 4 Signal sampled in the time domain

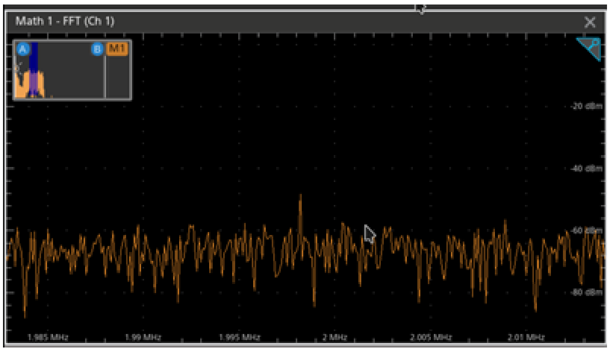

Figure 5 Signal from fig.4, converted in the frequency domain

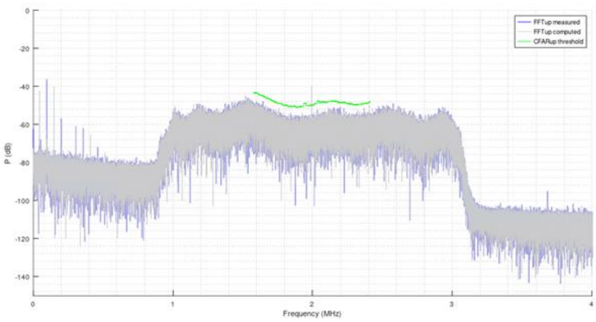

Figure 6 Signal from fig.4, converted in the frequency domain using the radar SP (N=262,144)

$$w_{STFT} = \frac{1}{B_{Rx}} = 50\ ms \qquad (6)$$

The calculation of a FFT with size N = 1,048,576 = 2^{20} requires a time of approximately 10ms by classical methods and approximately 1ms by parallel calculation.

The conditions regarding the necessary computational and time resources are met in the case of the space radars that work at very long distances, as the long distances impose the use of very low modulation or repetition frequencies.

4 RADAR ANTENNA CALIBRATION TEST

The present state of the commissioning is the antennas calibration. Each antenna has a gain of 63.5dBi and a beamwidth of 1.1 deg. This is a crucial test since both antennas have to be aligned with an error less than 25 mdeg for the radar to operate properly. Due to the size of the Cassegrain antennas (32m), their electromagnetic far field starts at more than 40 km away, making the classical measurement impractical. Combined with the scarcity of satellites transmitting in the C-band, the only viable option is to use radiostars. For the alignment, due to their strong flux, Taurus A and Cassiopeia A were chosen. As the line of sight theoretical values for the azimuth and elevation of the line of sight to these constellations can be precisely propagated, the alignment is expected to provide the required pointing precision.

The test set-up is presented in Figure 7. Each antenna is connected to a FSV3030 spectrum analyzer from Rohde & Schwarz through a LNA with 30 dB of gain. A laptop is used to retrieve the measurement data from the FSV3030. The analyzer is configured on the central

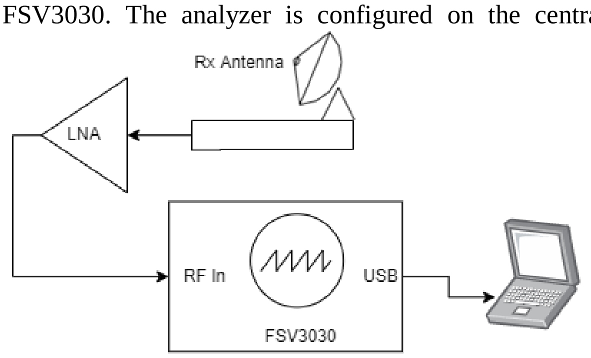

Figure 7 Antenna alignment setup

frequency 5,840 MHz and zero span, maximum resolution bandwidth, minimum video bandwidth and a sweep time > 50 s. The Program Track facility of the ACU is used for positioning the antenna under test towards the radiostar source. The received power level is continuously monitored on the spectrum analyzer. By using the “Adjust Offsets” functionality in the ACU, the maximum received power level is maintained by slightly offsetting the antenna clockwise/counter clockwise in azimuth and up/down in elevation.

Figures 8 and 10 show the variation of the received signal level for the Cheia 2 antenna as it is locked on Taurus A/Cassiopeia A position with a 0.5 deg step in azimuth from pointing towards the sky.

Figures 9 and 11 show the variation of the received signal level for the Cheia 2 antenna as it is locked on Taurus A/Cassiopeia A position with a 0.5 deg step in elevation from pointing towards the sky.

Figure 8 Received signal power from Cheia 2 as it is locked on Taurus (0.5 deg AZ step response)

Figure 9 Received signal power from Cheia 2 as it is locked on Taurus (0.5 deg EL step response)

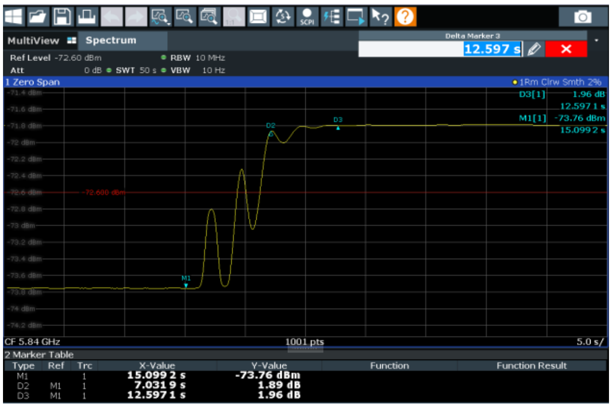

Figure 10 Received signal power from Cheia 2 as it is locked on Cassiopeia A (0.5 deg AZ step response)

5 CONCLUSIONS

This paper gives an overview of the Cheia Space Radar special design and its commissioning status. It describes the functional process of object tracking and details the operation of its signal processor, pointing out that, for the space radar field, the switching to frequency processing, instead of the classical time processing, can

Figure 11 Received signal power from Cheia 2 as it is locked on Cassiopeia A (0.5 deg EL step response)

offer substantial benefits. The most important benefit is the reduction of the transmitted power and the possibility of using Solid State Power Amplifiers, both providing an important reduction of the operational power consumption. The Radar antenna calibration procedure is presented and initial results are shown.

The work reported in this paper has been partly performed under a contract of the European Space Agency in the frame of the SSA P3-SST-V- Cheia Phase 2 (Tracking Radar retrofit for Cheia), within the European Space Operations Centre (ESOC).

6 REFERENCES

1. Ionescu L., Rusu-Casandra A., Bira C., Tatomirescu A., Tramandan I., Scagnoli R., Istriteanu D., Popa A.E., Development of the Romanian Radar Sensor for Space Surveillance and Tracking Activities. Sensors 2022, 22(9), 3546; 19 p, https://doi.org/10.3390/s22093546, ISSN: 1424-8220

2. Bira, C.; Rusu-Casandra A., A. Dataset of Spatial Objects Acquired Using Romania's First Ground-Based Space Tracking Radar. In Proceedings of the 14th International Conference on Communications COMM 2022, Bucharest, Romania, 16–18 June 2022.

3. Tatomirescu, A.; Rusu-Casandra A., C-Band FMCW RADAR Receiver Architecture for Space Debris Observation. In Proceedings of the 14th International Conference on Communications COMM 2022, Bucharest, Romania, 16–18 June 2022.

4. Tramandan, I; Rusu-Casandra A., Real-Time Monitoring and Command System for the Cheia Space Surveillance and Tracking Radar. In Proceedings of the ISETC 2022 Conference, Timisoara, Romania, November 2022

5. A.L. Lance, W.D. Seal, F. Labaar, Phase Noise and AM Measurements. Infrared and Milimetric Waves vol.11, Academic Press, 1984.
6. Sean Victor Hum, Noise in Radio Systems, Radio and Microwave Wireless Systems, University of Toronto,.
7. Jason Breitbarth, Joe Koebel, Additive (Residual) Phase Noise Measurement Of Amplifiers, Frequency Dividers And Frequency Multipliers, MICROWAVE JOURNAL, 2008
8. Radio noise, Recommendation ITU-R P.372-13, 2016
9. Alper Demir, Amit Mehrotra, and Jaijeet Roychowdhury, Phase Noise in Oscillators: A Unifying Theory and Numerical Methods for Characterization, IEEE Transactions on circuits and systems—I: Fundamental Theory and Applications, vol. 47, no. 5, may 2000
10. Bassem.R. Mahafza, Radar Systems Analysis and Design Using MATLAB, CHAPMAN & HALL/CRC, 2000
11. Barton, D. K., Modern Radar System Analysis, Artech House, Norwood, MA, 1988.
12. Edde, B., Radar - Principles, Technology, Applications, Prentice-Hall, Englewood Cliffs, NJ, 1993.